

Transient Symmetry Controls Photo Dynamics near Conical Intersections

Max D.J. Waters,[§] Wenpeng Du,[#] Andres Moreno Carrascosa,[#] Brian Stankus,[&] Martina Cacciarini,[‡] Peter M. Weber,[#] and Theis I. Sølling^{†,}*

[§]Laboratorium Für Physikalische Chemie ETH Zürich Vladimir-Prelogs-Weg 2, 8093 Zürich, Switzerland [#]Department of Chemistry Brown University Providence, RI 02912, United States of America

[&]Department of Chemistry and Biochemistry, Western Connecticut State University, Danbury, CT 06810, United States of America

[‡]Department of Chemistry, University of Florence, Via della Lastruccia 3-13, 50019 Sesto Fiorentino (FI) Italy

[†]College of Petroleum & Geosciences, King Fahd University of Petroleum & Minerals, Dharan 31261, Saudi Arabia email: theis.solling@kfupm.edu.sa

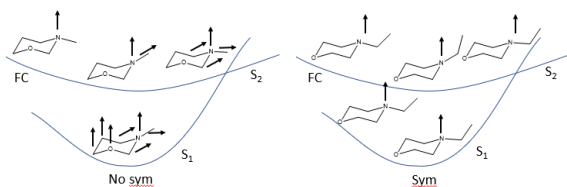
AUTHOR INFORMATION

Corresponding Author

Prof. Theis I. Sølling, College of Petroleum & Geosciences, King Fahd University of Petroleum Minerals, Dharan 31261, Saudi Arabia, email: theis.solling@kfupm.edu.sa

ABSTRACT Excited-state chemistry lacks generalised symmetry rules. With many femtochemistry studies focused on individual cases, it is hard to build up the same level of chemical intuition for excited-states as exists for ground states. Here, we unravel the degrees of freedom involved in ultrafast internal conversion (IC) by mapping the vibrational coherence of the initial wavepacket, and the dependence on molecular symmetry in various cyclic tertiary amines. Molecular symmetry plays an important role in the preservation of vibrational coherence in the transit from one electronic state to another. We show here that it is sufficient for the molecule to simply have the possibility of a more symmetric structure to achieve the preservation of vibrational coherence. It can be transient and still lead to preservation. This finding provides an additional angle on how symmetry influences electronic transitions and an additional piece to the puzzle of establishing symmetry-based selection rules for excited-state processes.

TOC GRAPHICS



The mere possibility of excited-state symmetry enables the preservation of vibrational coherence in a specific degree of freedom following a non-radiative transition that normally would be expected to be statistical in nature. *N*-ethyl morpholine undergoes fast internal conversion. Because of symmetry restrictions, the coherence of the amine wagging motion is retained in excited state structure outside of the Franck-Condon region. This stands in contrast to the asymmetric where there is no coupling restriction and thus no preservation of coherence. The arrows represent molecular vibrations. In the asymmetric system most of the molecular vibrations are active on the lower-lying state.

KEYWORDS Coherence • non-statistical • Ultrafast • Rydberg State • Photo electron spectroscopy.

Ultrafast internal conversion (IC), or rather, IC on a femtosecond timescale, is a topic of research that has gained much attention due to its fundamental role in directing photochemical dynamics.¹⁻

⁵ Central to this process are the conical intersections (CIs) – a point on the potential energy landscape where two potential energy surfaces are degenerate. A CI is often referred to as a photochemical funnel and is often characterized by the non-adiabatic coupling vector and the gradient difference vector, where the former constitute a favourable route to the symmetry of the coupling mode.⁶ CIs can efficiently mediate radiationless relaxation of an electronically excited molecule, of which IC is an example.⁶⁻⁹ Symmetry is a key tool to help predict and explain dynamical behaviour on ultrafast timescales.¹⁰⁻¹³ The following symmetry condition is useful in helping predict the symmetry of the coupling mode, and is helpful in predicting the appearance of certain kinds of CIs:

$$\Gamma_n \times \Gamma_Q \times \Gamma_m \supseteq \Gamma_A$$

If the direct symmetry product of the initial state Γ_n , the coupling mode Γ_Q , and the final state Γ_m , are a superset of the totally symmetric irreducible representation Γ_A , a CI is an allowed topographical feature on the potential energy hypersurface.⁶ The topology of the potential energy landscape surrounding a CI is theoretically described as a function of the perturbations to the molecular geometry following two degeneracy-lifting vectors: the gradient-difference mode, and the non-adiabatic coupling vector, which follows the symmetry that couples the electronic states (Γ_Q).^{6,14}

This theoretical description of a CI can be validated through the observation of vibrational coherence following ultrafast IC because the coherence often corresponds to the motion of the

vibronic wavepacket along one of the modes in the branching space of the CI.¹⁵⁻¹⁷ Vibrational coherence is an uncommon observation in large molecules because there are many vibrational degrees of freedom available and often very few symmetry restrictions. Intermode coupling can be reasonably expected to dissipate excess potential energy, resulting in a rapid loss of the coherence that is intrinsic to the initially prepared wavepacket. Nevertheless, preservation of vibrational coherence has recently been observed in cyclic tertiary aliphatic amines (CTAAs)^{18,19} and associated with symmetry restrictions of the available vibrational modes that can dissipate the energy.¹⁵ We demonstrate now that even the mere possibility of a symmetric conformation can control the fate of a photoexcited system to the extent that it is coherently funneled through a CI. To this end, we investigate a molecule that starts of in an asymmetric ground-state structure and ends in a symmetric equilibrium structure immediately after exciting the Franck-Condon region. This transition can take place on the ultrafast timescale without dissipation of the internal energy because the gradient at the Franck-Condon region directs the structural change towards the symmetric excited-state equilibrium structure. In the context of the Rydberg state dynamics of these CTAAs, the CI of interest is formed between the 3p manifold and the 3s Rydberg state. It has been established that the CI coupling space primarily can be described as more or less being in-line with (an extension of) the path from the Franck Condon geometry to the 3p equilibrium structure.¹⁵

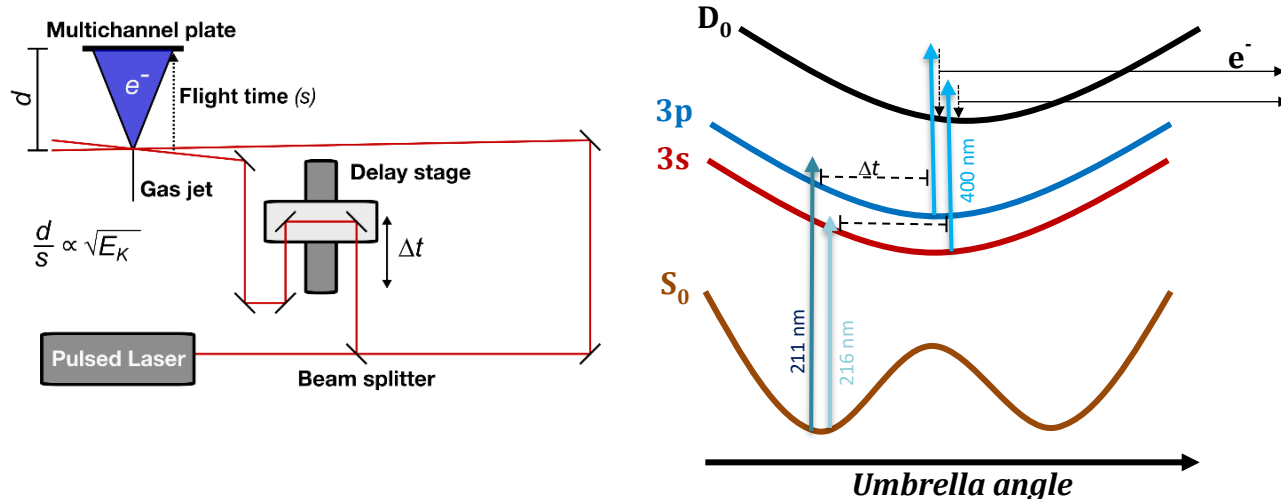


Figure 1. (Left) A generalised schematic for a pump-probe time-of-flight photoelectron spectrometer, where the time resolution is introduced through a moving stage which changes the length of one of the beam paths. The flight time of the photoelectrons is recorded, which is inversely proportional to the square root of the photoelectron kinetic energy. (Right) A cartoon of how pump-probe spectroscopic techniques can be mapped onto the potential energy landscape of a molecular system – in this case, CTAAAs which planarise around the nitrogen centre upon excitation to a Rydberg state, allowing us to obtain time-resolved measurements of chemical dynamics. The corresponding molecular motion can be thought of as being an amine wag which is populated because it is associated with the steepest descent out of the Franck-Condon region (movie in SI). Oscillatory motions are observable because of the fact that D_0 is slightly shifted from the Rydberg states.

We report time-resolved photoelectron spectra (TRPES) of three CTAAAs (setup and principle in Figure 1): *N*-methyl morpholine (NMM), *N*-ethyl morpholine (NEM), and *N*-methyl isomorpholine (NMI). A calculation (SI) shows that it is only the symmetry breaking conformer of NEM that is relevant to consider to begin with because it is more stable by 11 kJ/mol compared to the symmetric one (that resembles NMM). A schematic of the experimental technique, and how it allows us to extract dynamical information about molecular systems, is shown in Figure 1, and further details can be found in the supplementary information. The TRPES were measured at two different pump energies, 211 nm and 216 nm in order to probe the ultrafast dynamics in the region of the CI as closely as possible (the minimum energy structures are presented in Figure 2). A pump energy of 211 nm was chosen as this energy is enough to populate the 3p manifold in each of the three systems, whereas 216 nm is just below this threshold. At the longer pump wavelength, there is evidence for some 3p population (as can be seen in Figure 3.), because the Franck-Condon envelope is so large that the 3s and 3p spectral bands overlap, however it should be highlighted that the majority of the excited state population that is induced by 216 nm light is prepared on the 3s state, so the dynamics are dominated by the 3s state – even though we can extract and fit decay times of the 3p manifold when pumping with 216 nm. The probe wavelength for all measurements is 400 nm.

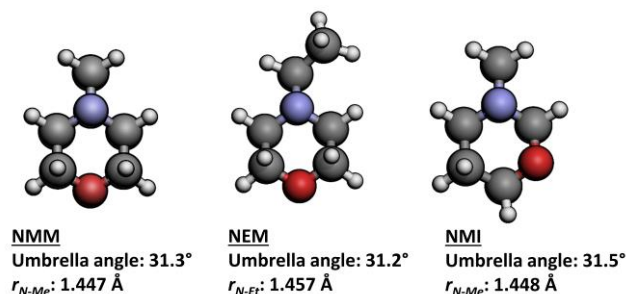


Figure 2. Geometries and selected parameters of the ground state optimised structures of NMM, NMI, and NEM, calculated at the CAM-B3LYP/6-311++G(d,p) level of theory. The umbrella angle is defined as the dihedral angle between the central nitrogen, and the three carbons bonded to it.

Figure 2. illustrates that NMM is the only molecule in this study that exhibits C_s symmetry in its ground electronic state, the calculated ground-state geometries of NMM and NMI are adapted from a previous study.¹⁵ Electronic excitation that involves a lone pair to Rydberg transition retains this symmetry as recent structure measurements of NMM in 3p and 3s have revealed.²⁰ Both NEM and NMI are C_1 in the ground state. The geometric parameters of the target molecules are all very similar. This structural similarity between the three systems makes them highly suitable for comparison, as it implies that the main difference between the molecules pertains to symmetry, and the inertia of the amine wagging motion.

Figure 3. shows the measured TRPES of the three molecules for two different pump wavelengths. It can be seen that each molecule shows vibrational coherence when excited by 216 nm. Coherent oscillations are also observed in NMM and NEM when pumped with a higher energy pulse (211 nm). However, the coherence is lost in NMI for the higher photon energy. These observations are consistent with previously published measurements.^{15,18,19} In the spectra measured with a 216 nm pump, NMI shows very little 3p photoelectron signal when compared to NEM and NMM. This means that the 3p state is not populated to a significant extent at 216 nm. Previously, the difference between NMM and NMI was assigned to symmetry selection rules restricting the number of

vibronic transitions that are allowed in NMM compared to NMI.¹⁵ NEM shows a similar 3p photoelectron binding energy to NMM and does give rise to an oscillating signal even though the ground electronic state molecular symmetry of NEM is C_1 . This implies that the symmetry restrictions on the initial allowed vibronic transitions do not tell the full story and further insights are necessary to explain the NEM dynamics.

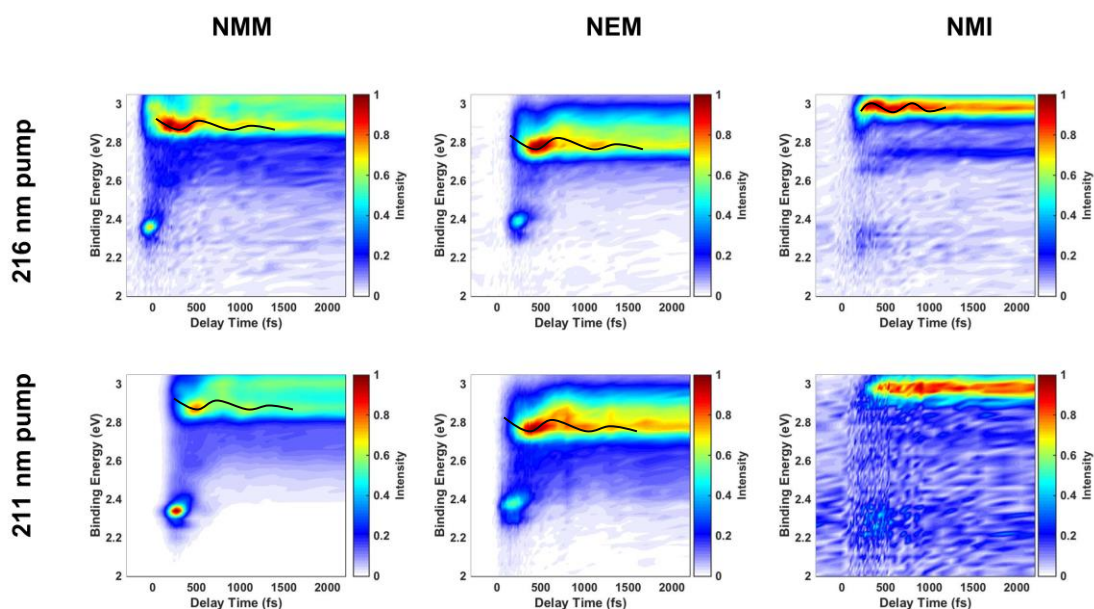


Figure 3. Time resolved photoelectron spectra for N-methyl morpholine (NMM), N-ethyl morpholine (NEM), and N-methyl isomorpholine (NMI), measured with two different pump wavelengths, 216 nm, and 211 nm, and probed with 400 nm light. In each spectrum, the photoelectron peak with the lowest binding energy, centered at 2.3 – 2.4 eV originates from the 3p Rydberg manifold, whereas the long-lived peak in the 2.8-3.0 eV range is the 3s signal. The guide was added in the first spectrum to make the oscillations more evident: They should be apparent in all but the last spectrum. It can be seen that NMI has by far the highest frequency oscillations.

The results of the fitting procedures are outlined in Table 1. We notice that the decay of the 3s state is outside our experimental range and that the lifetime has been fixed to a constant large value. The methodology is described in the supporting information, where the graphical representations of the fitting components for the 3s and 3p states of each molecule can also be found. The time constants returned by the fits of the 3p manifold in each system are shown in

Table 1 together with the oscillation period and damping time at each probe wavelength. It is important to realize that the wagging motion is launched in the Franck-Condon region in all molecules.

Looking at the decay time constants for the 3p Rydberg manifold for NEM and NMM pumped at 211 nm, it is seen that they both decay on comparable timescales (117 fs, and 120 fs, respectively), which is significantly faster than the decay of the NMI 3p Rydberg manifold (307 fs). These results are in good agreement with previously reported findings, which found that the 3p decay constants associated with NMM are in the range of 106-120 fs, 117 fs for NEM, and 312 fs for NMI.^{15,19} The fact that NEM and NMM have nearly identical decay times is highly surprising. Given that both molecules show long-lived vibrational coherence in the 3s state, statistical dynamics based on the density of states can be ruled out. Additionally, the ethyl group has significantly more mass compared to the methyl group (as is reflected by the longer oscillation period for the umbrella motion in the 3s state in NEM).

The short-lived 3p manifold of NEM, along with the preserved vibrational coherence in the 3s electronic state, implies that the dynamics of this molecule is ballistic and non-statistical – just as it is in NMM. This is somewhat surprising as the initial wavepacket is prepared in a similar number of vibronic states as that of NMI, due to the lack of symmetry in NEM at time zero. This surprising nonergodicity seen in NEM is highlighting the flaws in using statistical models to explain ultrafast behaviour. To further this, we wish to emphasise that adequate theoretical descriptions of ultrafast behaviour need to adapt to coupling conditions that will change as a function of the reaction coordinate, as it is fundamentally these coupling conditions (whether that is intermode coupling, or nonadiabatic coupling) that provide the various relaxation pathways. This is something that is

shown quite starkly in the case of NEM, because the symmetry that is introduced as a function of the relaxation coordinate hinders coupling between symmetric and non-symmetric vibrational modes.

Table 1. Fitting of the oscillation present in the 3s state and the lifetimes of the 3p state (errors are reported within the 95% confidence bounds).

Molecule	Pump Wavelength (nm)	3p residence time	Damping time (fs)	Period of Oscillation (fs)
NMM	216	104(6)	500(213)	650(80)
	211	125(5)	665(196)	600(39)
NEM	216	121(7)	490(120)	806(118)
	211	111(17)	412(126)	708(85)
NMI	216	242(76)	294(40)	373(23)
	211	298(133)	-	-

As is highlighted more quantitatively in Table 1, all three molecular systems show vibrational coherence in the amine wagging motion when directly excited to the 3s Rydberg state. Previous studies have reported oscillation periods of NEM and NMM when directly excited to the 3s state of 760(47) and 650(13) fs, respectively. This is in excellent agreement with the results presented here.^{18,19} The coherent oscillations arise because the amines tend to planarise when irradiated in such a way that an electron is promoted from the nitrogen lone pair to a Rydberg orbital.^{11,15,19,21} Furthermore, it has been firmly established that the amine wagging motion is the mode along which relaxation out of the Franck-Condon region occurs in these molecules, most recently by x-ray scattering measurements of the molecular structure of NMM in its 3s state.^{15,18–20} We note that the wagging frequency in the 3s state of NEM is half of what it is in NMI (Table S3, SI) and we propose that this is due to an unbalance in the asymmetric ring structure of NMI that allows for a wagging motion that is located mostly in one side of the system. This is in-line with the

experimental finding that the oscillation period in NMI is half of what it is in NEM. It is also worth noticing that all the low frequencies have an ethyl wagging component which does indeed make the symmetrization of NEM by the rotation of the ethyl group a very plausible process.

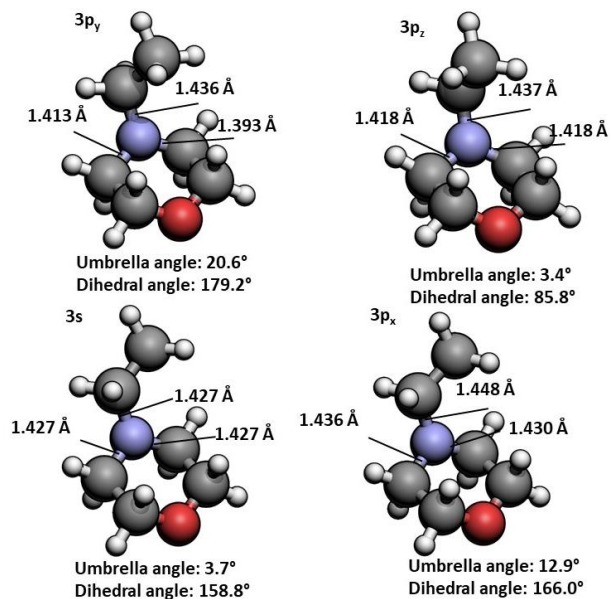


Figure 4. Calculated (CAM-B3LYP/6-311++G(d,p) level of theory) excited state minima for NEM in its 3p and 3s Rydberg states show that NEM only becomes symmetric in the 3p_z.

With the longer pump wavelength (where the molecules are excited to the 3s Rydberg state, with no ultrafast internal conversion being involved (before or after), the damping time for the amine wagging in NMI is ~294 fs. This is significantly shorter than the damping times for NEM and NMM, which are 412 fs and 665 fs, respectively. This can be rationalised by considering that no intermode coupling is explicitly forbidden for a molecule with C₁ symmetry. Therefore, the energy in the amine wagging motion will be able to dissipate to other vibrational modes much more efficiently than in molecules with symmetry restrictions that hinder intermode coupling. Another possible explanation could be dephasing of the wavepacket due to superposition of vibrations with

slightly different frequencies of different conformers. However, the relative energy of the ground state conformers (SI, Figure S5), this seems less likely that there are more than one conformeric species involved. Calculated excited state minimum energy geometries, Figure 4., show that the point group symmetry for the NEM molecule in its $3p_z$ state is C_s . Because of its large oscillator strength, the $n \rightarrow 3p_z$ state is the most populated state of the three $3p$ -states (CAM-B3LYP/6-311++G(d,p) predicts $f = 0.0156$ for the $3p_z$ state versus $f = 0.003$ for the two others).

The consequence of the excited state minima in the $3p_z$ state being C_s is that there will be a symmetry restriction on the energy dissipation through intermode coupling, and that the CI between the $3p_z$ state and the $3s$ state is allowed to form along normal modes that retain the mirror plane. In this case, the coupling space is made up of two symmetric amine wagging motions.

Given that NEM is C_1 in its ground state geometry, it could be expected that the excited state dynamics follows that of NMI, where the initially prepared wavepacket explores the potential energy surface of the $3p$ Rydberg state ergodically. However, NEM behaves like NMM and the vibrational coherence is observed to be preserved on the $3s$ state. A conical intersection was found along a direction that more or less is in-line with (an extension of) the path from the Franck Condon geometry to the $3p$ equilibrium structure. The structure is shown in Figure 5 and it can be seen that the coupling space essentially is defined by wagging motions (leading to flattening at N) and motions of the ethyl group. The energy of the CI is found to be 0.23 eV higher than that at the FC geometry but 0.91 eV lower than energy provided by a 211 nm photon which is taken to be consistent with the experimental 120 fs decay time of the $3p$ population. NMI, on the other hand, is proposed to explore the $3p$ surface more extensively due to the lack of symmetry restrictions. This is giving rise to the approximately three-times larger $3p$ lifetime in NMI. The insights provided by studying NEM demonstrate that the initial population seems in fact to be secondary as long as

the energetically favorable path out of the Franck Condon region introduces symmetry as is the case for NEM.

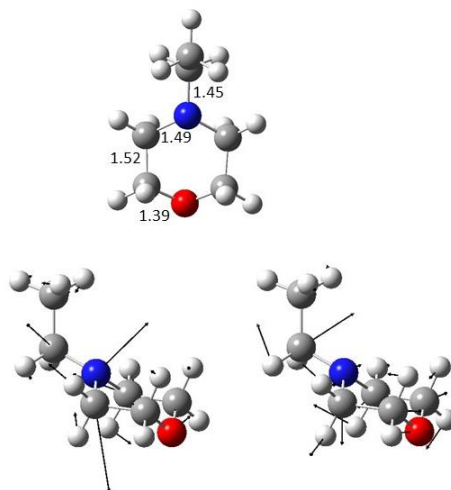


Figure 5. The conical intersection between the $3p_z$ and the $3s$ states. The top shows the structure with bond lengths in Angstroms and the bottom structures depict the non-adiabatic coupling vector (left) and the gradient difference (right). The ethyl group is perpendicular to the plane of the ring. The structure is calculated at the CAS(12,11)/aug-cc-pvdz level of theory with the BAGEL package.²² The energy of the CI is found to be 0.23 eV higher than that at the FC geometry but 0.91 eV lower than energy provided by a 211 nm photon.

In NMI, symmetry effects do not enter the dynamics at any point, because the molecular structure is always C_1 . However, in NEM, the energetically favored path involves an ethyl rotation during the Franck-Condon relaxation that leads to a structure with a mirror plane in the molecule. We attribute this rotation to a hyperconjugation effect that is only possible in the $3p_z$ state. This hyperconjugation occurs because electron density has been removed from the lone pair on nitrogen, creating an electron deficit in this orbital. The ethyl group then rotates, as this deficit can be stabilised through an attraction between the C-C σ bond and the partially filled lone pair.

In conclusion, NEM presents a case where, given the nature of the CI, the mere possibility of symmetry creates a dynamic funnel that leads to the preservation of coherence. This molecular system is demonstrating how transient symmetry can play a key role in the IC process, an important finding when a full set of symmetry rules are to be derived. The symmetry rules that are discussed here are general, but there are certain boundary conditions that will have to be in play when it comes to the potential energy surfaces that are involved. There will have to be a possibility of an ultrafast transition between two excited states that are involved and this transition will have to involve the degrees of freedom that are activated upon the exit from the Franck-Condon region. Interestingly, we have actually found that this condition has been fulfilled in all of the systems what we have studied hitherto.²³ Therefore, we have no reason to believe that the symmetry findings are not general.

ASSOCIATED CONTENT

Supporting Information.

The following files are available free of charge.

Detailed experimental description, computational details and data analysis.

Extended results (six figures, eight tables and one movie)

AUTHOR INFORMATION

Notes

The authors declare no competing financial interests.

ACKNOWLEDGMENT

MDJW thanks the Danish Chemical Society for their support through the Kemisk Forenings Rejsefond (Grant No. J.n.r 2018-15). Parts of this project (PMW) were funded by the Army

Research Office, Award # W911NF-19-1-0178, and the U.S. Department of Energy, Office of Science, Basic Energy Sciences, under Award # DE-SC0017995 and DE-SC0020276.

REFERENCES

- (1) Polli, D.; Altoe, P.; Weingart, O.; Spillane, K. M.; Manzoni, C.; Brida, D.; Tomasello, G.; Orlandi, G.; Kukura, P.; Mathies, R. A.; Garavelli, M.; Cerullo, G. Conical Intersection Dynamics of the Primary Photoisomerization Event in Vision. *Nature* **2010**, *467* (7314), 440-443.
- (2) Molnar, F.; Ben-Nun, M.; Martínez, T. J.; Schulten, K. Characterization of a Conical Intersection between the Ground and First Excited State for a Retinal Analog. In *Journal of Molecular Structure: THEOCHEM*; 2000.
- (3) Worth, G. A.; Cederbaum, L. S. Mediation of Ultrafast Electron Transfer in Biological Systems by Conical Intersections. *Chem. Phys. Lett.* **2001**, *338* (4–6), 219–223.
- (4) Olaso-González, G.; Merchán, M.; Serrano-Andrés, L. Ultrafast Electron Transfer in Photosynthesis: Reduced Pheophytin and Quinone Interaction Mediated by Conical Intersections. In *AIP Conference Proceedings*; 2007.
- (5) Solling, T. I.; Kuhlman, T. S.; Stephansen, A. B.; Klein, L. B.; Moller, K. B. The Non-Ergodic Nature of Internal Conversion. *Chemphyschem* **2014**, *15* (2), 249–259. <https://doi.org/10.1002/cphc.201300926>.
- (6) Koppel, H.; Domcke, W.; Cederbaum, L. Multimode Molecular-Dynamics Beyond the Born-Oppenheimer Approximation. *Adv. Chem. Phys.* **1984**, *57*, 59–246.
- (7) Yarkony, D. R. Diabolical Conical Intersections. *Rev. Mod. Phys.* **1996**, *68* (4), 985–1013.
- (8) Domcke, W.; Yarkony, D. R. Role of Conical Intersections in Molecular Spectroscopy and Photoinduced Chemical Dynamics. In *Annual Review of Physical Chemistry, Vol 63*; Johnson, M. A., Martinez, T. J., Eds.; Annual Reviews: Palo Alto, 2012; Vol. 63, pp 325–352.
- (9) Schuurman, M. S.; Stolow, A. Dynamics at Conical Intersections. In *Annual Review of Physical Chemistry, Vol 69*; Johnson, M. A., Martinez, T. J., Eds.; Annual Reviews: Palo Alto, 2018; Vol. 69, pp 427–450.
- (10) Dereka, B.; Svehkarev, D.; Rosspeintner, A.; Aster, A.; Lunzer, M.; Liska, R.; Mohs, A. M.; Vauthey, E. Solvent Tuning of Photochemistry upon Excited-State Symmetry Breaking. *Nat. Commun.* **2020**, *11* (1), 1925.
- (11) Svoboda, V.; Wang, C.; Waters, M. D. J.; Woerner, H. J. Electronic and Vibrational Relaxation Dynamics of NH₃ Rydberg States Probed by Vacuum-Ultraviolet Time-Resolved Photoelectron Imaging. *J. Chem. Phys.* **2019**, *151* (10), 104306.
- (12) Boguslavskiy, A. E.; Schuurman, M. S.; Townsend, D.; Stolow, A. Non-Born-Oppenheimer Wavepacket Dynamics in Polyatomic Molecules: Vibrations at Conical Intersections in DABCO. *Faraday Discuss.* **2011**, *150*, 419–438.
- (13) Pertot, Y.; Schmidt, C.; Matthews, M.; Chauvet, A.; Huppert, M.; Svoboda, V.; von Conta, A.; Tehlar, A.; Baykusheva, D.; Wolf, J.-P.; Worner, H. J. Time-Resolved x-Ray Absorption Spectroscopy with a Water Window High-Harmonic Source. *Science* **2017**, *355* (6322), 264-267.

- (14) Matsika, S.; Krause, P. Nonadiabatic Events and Conical Intersections. In *Annual Review of Physical Chemistry, Vol 62*; Leone, S. R., Cremer, P. S., Groves, J. T., Johnson, M. A., Eds.; Annual Reviews: Palo Alto, 2011; Vol. 62, pp 621–643.
- (15) Waters, M. D. J.; Skov, A. B.; Larsen, M. A. B.; Clausen, C. M.; Weber, P. M.; Sølling, T. I. Symmetry Controlled Excited State Dynamics. *Physical Chemistry Chemical Physics* **2019**, *21*, 2283–2294.
- (16) Hoffman, D. P.; Ellis, S. R.; Mathies, R. A. Characterization of a Conical Intersection in a Charge-Transfer Dimer with Two-Dimensional Time-Resolved Stimulated Raman Spectroscopy. *J. Phys. Chem. A* **2014**, *118* (27), 4955–4965.
- (17) Worth, G. A.; Welch, G.; Paterson, M. J. Wavepacket Dynamics Study of Cr(CO)(5) after Formation by Photodissociation: Relaxation through an (E Circle plus A) Circle Times e Jahn-Teller Conical Intersection. *Mol. Phys.* **2006**, *104* (5–7), 1095–1105.
- (18) Zhang, Y.; Jonsson, H.; Weber, P. M. Coherence in Nonradiative Transitions: Internal Conversion in Rydberg-Excited N-Methyl and N-Ethyl Morpholine. *Physical Chemistry Chemical Physics* **2017**, *19* (38), 26403–26411.
- (19) Zhang, Y.; Deb, S.; Jonsson, H.; Weber, P. M. Observation of Structural Wavepacket Motion: The Umbrella Mode in Rydberg-Excited N-Methyl Morpholine. *J. Phys. Chem. Lett.* **2017**, *8* (16), 3740–3744.
- (20) Stankus, B.; Yong, H.; Zotev, N.; Ruddock, J. M.; Bellshaw, D.; Lane, T. J.; Liang, M.; Boutet, S.; Carbajo, S.; Robinson, J. S.; Du, W.; Goff, N.; Chang, Y.; Koglin, J. E.; Minitti, M. P.; Kirrander, A.; Weber, P. M. Ultrafast X-Ray Scattering Reveals Vibrational Coherence Following Rydberg Excitation. *Nature Chemistry* **2019**, *11* (8), 716–721.
- (21) Gosselin, J. L.; Minitti, M. P.; Rudakov, F. M.; Solling, T. I.; Weber, P. A. Energy Flow and Fragmentation Dynamics of N,N-Dimethylisopropylamine. *Journal of Physical Chemistry A* **2006**, *110* (12), 4251–4255.
- (22) BAGEL, Brilliantly Advanced General Electronic-structure Library. Available at <http://www.nubakery.org> under the GNU General Public License.
- (23) Sølling, T. I.; Moller, K. B.; Stephansen, A. B.; Kuhlman, T. S.; The Non-Ergodic Nature of Internal Conversion. *ChemPhysChem.* **2014**, *15*, 249–259.